Electromodulation of charge-transfer photoexcitations in pristine and C_{60}-doped conjugated polymers

M. Liess* and Z. V. Vardeny
Department of Physics, University of Utah, Salt Lake City, Utah 84112

P. A. Lane
Department of Physics and Astronomy, University of Sheffield, Sheffield S3 7RH, United Kingdom
(Received 28 May 1998)

We study the effect of an electric field of up to 100 kV/cm on photoexcitations in pristine and C_{60}-doped π-conjugated polymers by electromodulated photoinduced absorption (EPA). In EPA, we measure changes in the photoinduced absorption of a polymer film induced by an electric field. The dominant effect is a change in the photoexcitation recombination kinetics, which leads to reduction or enhancement of the PA bands. We found that the electric field increases the decay rate of charge-transfer excitations; exciton dissociation near defects and impurities was also enhanced. A Stark shift of the photoexcitation energy levels for C_{60}-doped poly(*para*-phenylene) was also detected. From the EPA we calculate that the polarizability of the charge-transfer excitations in this blend is of order $3\times10^7(\text{Å})^3$. This is two orders of magnitude larger than the polarizability of the $1B_u$ exciton in most luminescent conjugated polymers. [S0163-1829(99)10715-X]

I. INTRODUCTION

Electromodulation spectroscopy is a valuable tool for studying photophysics of organic semiconductor. In particular, electroabsorption (EA) and electroreflectance have been widely used to understand the electronic structure of molecular semiconductors and π-conjugated polymers.[1–6] The EA spectrum has been ascribed to a combination of a Stark shift and symmetry breaking of molecular excitons by the electric field perturbation. The Stark shift produces a spectrum proportional to the first derivative of the absorption spectrum and symmetry breaking induces absorption bands from normally forbidden transitions. Oscillatory features have been obseved in the EA spectra of crystalline films of polydiacetylene[1] and explained by a Franz-Keldysh effect at the band edge. Electromodulated fluorescence has shown that an electric field alters both the dynamics and radiative yield of singlet excitons[7] due to field-induced dissociation of molecular excitons into charge carriers. Electromodulated fluorescence from organic molecules has been understood in terms of a Stark shift[8] or electric field induced dissociation of excitons into mobile charge carriers[9,10] in different configurations and materials. Models combining migration of molecular excitons combined with either intramolecular[11] or intermolecular[12] dissociation mechanisms have been proposed for π-conjugated polymers.

Photoinduced absorption (PA) spectroscopy has been employed to understand the nature of photoexcitations in semiconductors. When ultrafast pulsed lasers are used, the dynamics and spectra of singlet excitons with subnanosecond lifetimes can be measured. Photoexcitations such as triplet excitons, polarons, and polaron pairs have lifetimes greater than a microsecond and can be studied with a cw light source. As the PA spectrum includes contributions from multiple photoexcitations, it can be difficult to interpret the PA spectrum. Magnetic resonance spectroscopy is one way to separate out contributions of different excitations to the PA spectrum.[13] In this paper we will show that an applied electric field can also be used to elucidate the nature of photoexcitations responsible for the PA spectrum.

We have developed a kind of electromodulation spectroscopy to study charge-transfer photoexcitations in π-conjugated polymers: electromodulated photoinduced absorption (EPA). In EPA the sample is continuously illuminated by an above-gap pump beam and a probe beam; the PA is modulated by an applied electric field. While we observed no effect on triplet excitons and isolated polarons, the PA of charge-transfer excitations was found to be quite sensitive to the applied electric field. In combination with complementary spectroscopies, EPA aids us in elucidating the origin of the PA spectrum. Our measurements emphasize C_{60}-doped π-conjugated polymers, as doping produces a high concentration of long-lived photoexcitations. Excitons which diffuse close to a C_{60} molecule transfer a negative charge to the C_{60} molecule, leaving a positive polaron on the polymer chain. These charge-transfer excitations are similar to polaron pairs[14] in that their absorption signature is a combination of the absorption spectra of intrachain polaron pairs and C_{60} anions.[15,16] We present a detailed study of the effect of electric fields on these charge-transfer complexes.

Photoinduced charge transfer in C_{60}-doped π-conjugated polymer films was reported in 1992 and explained by ultrafast charge transfer to C_{60} from the polymer.[17–19] Sariciftci *et al.*[20–22] measured blends containing equal weights of C_{60} and poly(2-methoxy,5-(2′-ethyl-hexyloxy)-*para*-phenylene vinylene) (MEH-PPV), roughly one C_{60} molecule per three polymer repeat units. The fluorescence lifetime was reduced to below the 60 ps system resolution, the PL quantum yield was reduced by three orders of magnitude, and the photoconductivity was comparably enhanced. As a consequence of the high electron affinity of C_{60}, photogenerated excitons on the polymer chains dissociate when encountering C_{60} molecules. Based on the fluorescence lifetime, they estimate charge transfer occurs within a picosecond. Breuning and Friedman proposed a model for the charge transfer pro-

 ©1999 The American Physical Society

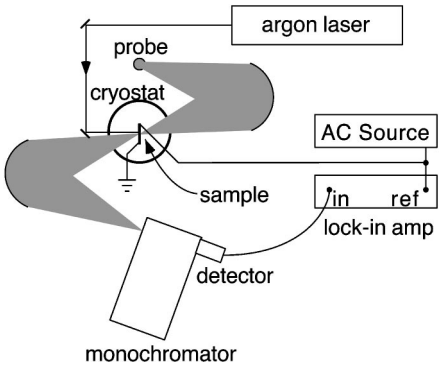

FIG. 1. A schematic diagram of the PA and EPA spectrometer. For PA measurements, the lock-in amplifier is referenced to an optical modulator placed in the laser beam path.

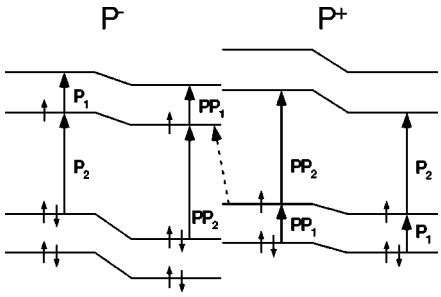

FIG. 2. A schematic diagram of the energy levels and optical transitions of isolated polarons (far left and far right) and a polaron pair (center).

cess for a polymer chain coupled to a C_{60} molecule.[23] They describe oscillatory behavior with a charge-transfer time of 200 to 300 fs, in agreement with the experimental estimate.

The paper has the following outline. In Sec. II, we describe the experimental techniques used in this work and explain how we interpreted the spectra. EPA measurements of pristine and C_{60}-doped MEH-PPV are discussed in Sec. III and we show that the EPA spectrum can be explained by field-assisted tunneling of charge from the C_{60} anion to the polymer chain. Sections IV and V describe EPA measurements of polythiophene and of C_{60}-doped dialkoxy poly(*para*-phenylene) (RO-PPP), respectively. We then summarize our results and conclude.

II. EXPERIMENTAL METHOD

A. Spectroscopy

Our study encompasses three related techniques: PA, EPA, and PA-detected magnetic resonance (PADMR). A schematic diagram of the PA spectrometer used in this study is shown in Fig. 1.[24] PA spectroscopy uses two beams; photoexcited states are generated by an above-gap pump beam and the probe beam measures the changes ΔT in the transmission T. The pump beam was generated by an argon ion laser, the 353 nm line was used to excite RO-PPP, and the 488 nm line was used to excite all other samples. The sample was placed in a cryostat equipped with sapphire or CaF_2 windows to permit measurements over a wide wavelength range at temperatures between 80 and 300 K. By the use of multiple monochromator gratings and IR detectors, we could measure PA in the spectral range from 0.1 to 3.5 eV. Transmitted light from the probe beam and fluorescence from the sample is dispersed through a 1/4 meter monochromator onto a photodiode. The normalized changes in transmission $-\Delta T/T \propto N\sigma d$, where N is the photoexcitation density, σ is the absorption cross section, and d is the sample thickness. The pump beam intensity is modulated by an acousto-optic modulator and the use of standard phase-sensitive lock-in techniques yields a signal resolution as low as 10^{-6}. In a typical experiment, the absorbed flux from the laser is about 2×10^{18} photons/cm^2 sec and the modulation frequency was 400 Hz. The samples used are thin polymer films spun-cast on sapphire or quartz substrates.

We are interested in the optical transitions of charged photoexcitations in π-conjugated polymers. Upon adding a charge to the polymer chain by chemical doping or photoexcitation, a structural relaxation shifts the HOMO and the now singly occupied SOMO level into the gap, resulting in the energy diagram for a negative polaron on the far left of Fig. 2. There is a similar shift of energy levels for a positive polaron, shown on the far right of Fig. 2. This combination of charge and structural distortion is referred to as a polaron and is analagous to anions and cations for molecules.[25] The parity of these levels alternates between even and odd, resulting in two allowed transitions (P_1 and P_2) and one forbidden transition.[26] The energy of the P_1 transition may be slightly different for positive and negative polarons due to charge conjugation symmetry violation.[27] When two polarons of opposite sign interact, the mutual Coulomb attraction shifts the energy levels of the two polarons, resulting in the schematic diagram shown in the center of Fig. 2. The higher-energy transition of the pair (PP_2) is blueshifted with respect to the P_2 transition of polarons. While a new transition could appear, this transition is likely to be weak for a long-lived polaron pair. Transitions of triplet excitons from the lowest triplet state (T_1) to higher lying triplet states (T_n) can also contribute to the PA spectrum. Studies of π-conjugated polymers have shown that only the $T_1 \rightarrow T_2$ transition lies below the optical gap.[13,28,29]

For EPA spectroscopy, the sample substrate was patterned with an array of interpenetrating gold electrodes before spinning of the polymer film. The spacing between the electrodes was 40 μm and a potential difference was applied to produce an electric field between 10^4 and 10^5 V/cm. The sample is continuously illuminated by both the pump and probe beams and transmission of the probe beam is modulated by the ac electric field. The signal is detected by a lock-in amplifier referenced to the second harmonic $2f$ of the electric field modulation frequency ($f=217$ Hz). As with PA, this signal is then normalized by the unmodulated transmission spectrum ($-\delta T/T$). We note a related paper which showed an optical switch could be built by modulating intersubband absorption of photogenerated electrons and holes in multiple quantum wells.[27]

PADMR measures the change in PA due to magnetic resonance.[28] The sample was mounted in a high-Q microwave cavity equipped with optical windows and a superconducting magnet. As with EPA, the sample is continuously illuminated by the pump and probe beams. Microwave resonant absorption leads to small changes in the transmission of the probe beam. Small changes δN in the photoexcitation density N are produced by microwave-induced transitions

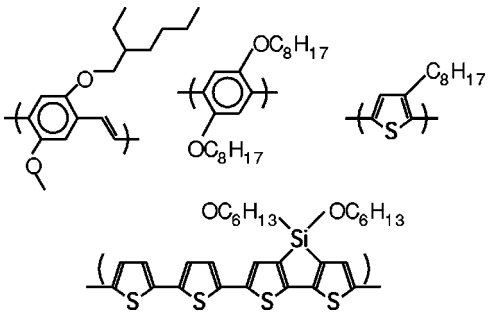

FIG. 3. Chemical structures of the π-conjugated polymers studied.

that change spin-dependent recombination rates. The PADMR spectra were measured at 10 K at a microwave frequency of 3 GHz and magnetic fields $H \approx 500$ G($\Delta m_S = 2$) for triplet excitons and $H \approx 1070$ G($\Delta m_S = 1$) for charged photoexcitations. The measurements allow us to determine the spin quantum number of photoexcitations and their PA spectra.[28]

We studied pure or C_{60}-doped films of MEH-PPV, poly(3-octylthiophene) (P3OT), silicon-bridged polythiophene (PTSi), and poly(2,5-dialkoxy *para*-phenylene) (RO-PPP). The repeat units of these polymers are shown in Fig. 3. Films were prepared by dripping solution containing the polymer alone or a mixture containing 0.3 mol C_{60} onto a sapphire substrate and evaporating the solvent in a vacuum. Since these measurements were done in the IR spectral range where the intrinsic absorption of most polymer films is weak, films of an optical density of up to 2 could be used. After fabrication the sample is kept in the dark in a dynamic vacuum of 10^{-3} Torr to avoid photo-oxidation.

B. Analysis of the EPA spectrum

A small change δT in transmission T can be expressed to first order as

$$\delta T = \frac{\partial T}{\partial n}\delta n + \frac{\partial T}{\partial \kappa}\delta \kappa, \tag{1}$$

where n and κ are the real and imaginary parts of the refractive index of the material, respectively. Normalizing the change in transmission δT by the transmission signal T, we get[30]

$$-\frac{\delta T}{T} = C_1 \delta n + C_2 \delta \alpha + \delta \alpha d, \tag{2}$$

where C_1 and C_2 are constants, $\delta\alpha$ is the induced change in the absorption coefficient and d is the thickness of the film. It can be shown[31] that the effect of the first two terms, which are induced by a modulation of the refractive index, is small compared to $\delta\alpha d$ and thus can be neglected. This is especially true in the spectral region below the optical gap. Consequently,

$$-\frac{\delta T}{T} = \delta \alpha d = \delta N \sigma d, \tag{3}$$

where N is the density of photoexcitations and σ is their absorption crosssection. Not all photoexcitations are similarly modulated. In case of a modulation of N by the applied electric field **F**, the EPA signal $(-\delta T/T)$ divided by the PA signal $(-\Delta T/T)$ gives the relative sensitivity of the photoexcitations to **F**

$$\frac{\delta T}{\Delta T} = \frac{\delta N}{N}. \tag{4}$$

Therefore, Eq. (4) can help to distinguish the contributions of various photoexcitations to the PA spectrum since the ratio $\delta T/\Delta T$ should be constant for the same excitation over a given photon energy range. Consider an EPA spectrum made up of contributions from several different photoexcitations. If a given EPA band is due to the electromodulation of the recombination kinetics of a given photoexcitation i, then the phase $\phi_i(\omega)$ of the EPA band is related to the excitation lifetime τ_i. If $\tau_i \ll 1/f$, where f is the modulation frequency of the electric field, no phase shift will be observed. In other words, N will follow the electric field modulation. A phase shift of $\phi(\omega) = \pi/2$ is reached if $\tau_i \gg 1/f$ (N lags the electric field). In general, the phase does not only indicate the process [electromodulated enhancement of the absorption if $\phi(\omega) < \pi$, electromodulated bleaching if $\phi(\omega) > \pi$], but it also gives information about the excitation lifetime. The phase information can also help to correlate different PA bands with one another. If the two PA bands are due to the same excitation, then the EPA bands should have the same phase.

The EPA spectrum can be disturbed by artifacts due to resistive heating, a Stark shift of the absorption edge due to an electric field (electroabsorption), and Thomas-Fermi screening of the electric field by charge carriers. We neglect the effect of resistive heating of the film, since thin films with a good heat contact to the substrate and a high resistance were used.[31] We have seen the Stark shift of the absorption edge in several films, but comparison of the EPA spectrum to the EA spectrum allows us to account for this effect. This means that a pure EPA spectrum can be observed only below the absorption edge. Similar difficulties lie in observing a pure PA spectrum above E_{gap} as charged photoexcitations generate an internal electric field which in turn produces a derivative-shaped spectrum.[32,33] Thomas-Fermi screening does not alter the EPA spectrum, but modulates its magnitude. A screening effect can lead to a sublinear dependence of the EPA signal δT on the pump intensity I.[31]

III. EPA SPECTROSCOPY OF MEH-PPV

A. Experimental results

The PA spectra of pristine MEH-PPV and the MEH-PPV/C_{60} composite are shown in Fig. 4(a). The dominant PA band of pristine MEH-PPV arises from optical transitions in triplet manifold $T_1 \rightarrow T_2$.[28] The PA band associated with charged photoexcitations in pristine MEH-PPV below 0.5 eV is very weak (4×10^{-5}), as seen previously.[34] In contrast, the PA spectrum of MEH-PPV/C_{60} is dominated by two bands with onsets at 0.25 eV (LE) and 1.18 eV (HE), respectively.[35] These two PA bands have the same intensity and modulation frequency dependence and are hence correlated.[34] The strong photoinduced infrared-active vibration (IRAV) modes below 0.2 eV are also correlated with the

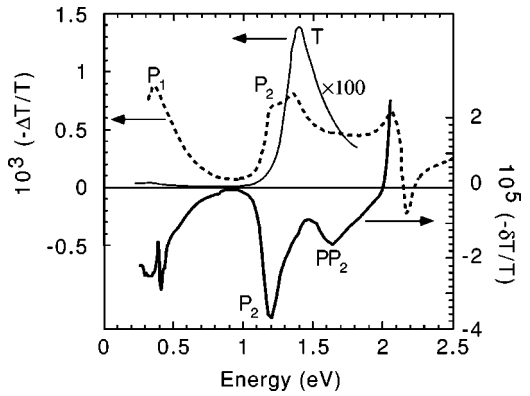

FIG. 4. Top, left axis: PA spectra of MEH-PPV (solid line) and MEH-PPV/C_{60} (dashed line). Bottom, right axis: EPA spectrum of MEH-PPV/C_{60}.

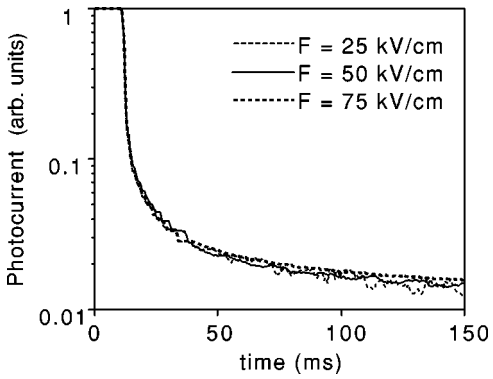

FIG. 5. Transient photocurrent in MEH-PPV/C_{60} at three different field strengths. The decay of the photocurrent is measured after the pump beam is shut off at $t=10$ ms.

LE and HE bands. As IRAV modes are due to the presence of charge on the polymer chains,[35] then the PA spectrum of C_{60}/MEH-PPV is due to charged photoexcitations. Indeed, previous PADMR measurements have shown that these exciations are polarons.[36] The derivative-shaped features with a zero crossing at 2.2 eV has the same line shape as the EA spectrum of MEH-PPV (Ref. 6) and is thus due to electric fields of photogenerated charged excitations. Despite the high concentration of C_{60}, we do not see the sharp PA band of C_{60}^- at 1.15 eV.[37]

The EPA spectrum of the MEH-PPV/C_{60} composite, shown in Fig. 4(b), consists of bands at 0.4, 1.18, and 1.65 eV, respectively. All three EPA bands are correlated by their dependence on the electric field strength and modulation frequency, as well as the pump beam intensity. Notably, the EPA bands are much narrower than the PA bands. The two high-energy EPA bands are distinct whereas the PA bands are spread out over a broader energy range. Above 2 eV, the EPA spectrum is dominated by electroabsorption. In order to be certain that the EPA spectrum results from electromodulated PA, we measured the EA spectrum at photon energies above and below the optical gap. No signal was observed at energies below 2.2 eV; the signal above this energy results from EA and has been discussed in detail elsewhere.[6] We tentatively assign the EPA bands at 0.4 and 1.65 eV to transitions of positive polarons on the polymer chains and the EPA band at 1.18 eV to C_{60}^-.

We also attempted to measure EPA in undoped MEH-PPV,[15] but detected no signal below the gap and the usual EA spectrum above the gap. This is not surprising as the PA spectrum of MEH-PPV shown above is dominated by triplet excitons. Warman *et al.*[38] recently compared the polarizabilities α_p of singlet and triplet excitons by time-resolved microwave conductivity measurements. They found that the polarizability change of singlet excitons in MEH-PPV $\Delta V_P = 2000$ Å^3, whereas for triplet excitons in polythiophene derivatives $\Delta V_P = 25$ Å^3. This is consistent with ODMR studies which have shown that triplet excitons are highly localized[39], with the triplet localized to a single phenyl ring. As the response to an applied electric field is proportional to the difference in polarizability between the ground and excited states, we expect any EPA from triplet excitons to be small. No EPA spectrum related to charge photoexcitations or charge transfer complexes was detected. The PA spectrum is of order 10^{-5} and the EPA signal in MEH-PPV/C_{60} is two orders of magnitude weaker than the PA itself. Hence, while we cannot exclude the possibility of any EPA in MEH-PPV, the signal is too weak to be detected.

We must also eliminate the possibility that the electromodulation signal is related to an effect of the electric field on the photocurrent (PC). The transient PC in the MEH-PPV/C_{60} composite generated by a 200 ms pump pulse of 100 mW at 488 nm is shown in Fig. 5. The PC decay was measured with fields of 0, 25, 50, and 75 kV/cm and the PC decay curves are normalized to one another to permit direct comparison. The PC decay is independent of the electric field strength, whereas the EPA signal is proportional to the square of the electric field (see below). Hence, the lifetime of optically induced charge carriers is not influenced by an electric field in MEH-PPV/C_{60}. These measurements show that the density of mobile charge carriers, and consequently their PA spectra, is not influenced by the applied electric field. In addition, charge transfer from the polymer to C_{60} appears to be independent of an applied field.

Finally, we show that the EPA signal is due to an electromodulation of the photoexcitation recombination kinetics in the MEH-PPV/C_{60} composite. Figure 6 shows the transient PA of C_{60}^- at 1.18 eV, plotted as $\ln(\Delta T)$ vs time (in milliseconds) for dc electric field strengths of 0, 25, 50, and 75 kV/cm. As the field strength increases, the PA decays more quickly due to a reduction in the lifetime (and hence the density) of immobile C_{60}^-. The time constant for the initial decay (within 1 ms) decreases from 1.4 to 1.2 ms as the electric field strength increases. Taken together, all of these

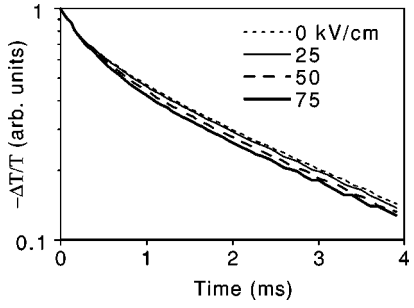

FIG. 6. Transient PA of MEH-PPV/C_{60} for electric fields between 0 and 75 kV/cm.

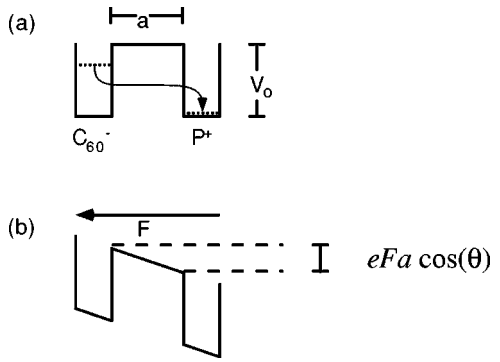

FIG. 7. (a) The model for an electron tunneling from C_{60}^- to a positive polaron. (b) The potential well in the presence of an applied electric field.

measurements are consistent with our conclusion that the EPA signal is due to electromodulation of photoexcitations in the MEH-PPV/C_{60} composite, i.e., electromodulated photoinduced absorption. An EPA signal can only be seen in the MEH-PPV/C_{60} composite under illumination. In this case a large number of charge transfer complexes (P^+/C_{60}^-) are present in the material. Absent doping or illumination, there will be no charge transfer complexes. Figure 5 showed that the effect of an electric field on the lifetime of mobile charge carriers and thus their contribution to the EPA spectrum can be ignored. We therefore conclude that the EPA signal must be due to charge transfer complexes.

B. Field-induced tunneling in the MEH-PPV/C_{60} composite

We now proceed to show that the increased recombination rate of charge transfer complexes in MEH-PPV/C_{60} blends is due to an electric field enhanced tunneling of the negative charge on the C_{60}^- back to the polymer chain. Figure 7 illustrates our model for an electron tunneling from the C_{60}^- through a potential barrier back to the polymer chain. The potential barrier has a height V_0 and width a and the angle between the electric field and the dipole moment of the charge-transfer complex is θ. The potential $V(x,\theta)$ can then be written

$$V(x,\theta)=V_0+efx\cos\theta. \tag{5}$$

The tunneling probability $\tilde{T}$ for an electron through this potential barrier is given by the WKB approximation

$$\ln\tilde{T}=-\sqrt{\frac{8m}{\hbar}}\int_0^a dx\sqrt{V_0+eFx\cos\theta}, \tag{6}$$

where m is the effective mass of the electron. It is possible that the width of the charge transfer complex itself may be modulated by elastic deformation. In the following simple model, we neglect these considerations. Integration of Eq. (6) yields

$$\ln\tilde{T}=-\frac{\sqrt{8m}}{3e\hbar F\cos\theta}[(V_0+eFa\cos\theta)^{3/2}-V_0^{3/2}]. \tag{7}$$

For a separation of a few nm, the difference in potential due to the electric field $\Delta V\leqslant eFa$ is of order 10 meV. This is obviously much smaller than the height of the potential barrier. Therefore, we perform a Taylor's series expansion to get

$$\ln\tilde{T}=-\sqrt{8ma^2V_0/\hbar^2}\left(1+\frac{eFa\cos\theta}{4V_0}\right). \tag{8}$$

We can rewrite Eq. (8) in terms of $\tilde{T}_0$, the tunneling probability absent the electric field:

$$\tilde{T}=\tilde{T}_0\exp(-\gamma eFa\cos\theta), \tag{9}$$

where $\gamma=\sqrt{ma^2/2V_0\hbar^2}$. We must take into account that the charge transfer complexes in a real film will be oriented randomly with respect to the electric field. As the electric field is a small perturbation to the potential, we can expand Eq. (9) in a Taylor's series and integrate θ over all possible angles. Any odd terms must vanish by parity and to lowest order:

$$\tilde{T}=\tilde{T}_0\left(1+\frac{ma^4e^2}{4V_0\hbar^2}F^2\right). \tag{10}$$

Thus, the application of an electric field always increases the tunneling probability and the effect is proportional to the square of the field strength. We experimentally verified this result by measuring the EPA signal δT as a function of the voltage across the sample (Fig. 8). This relation holds over two orders of magnitude of different pump illumination intensities and is independent of the pump power, and hence, the photoexcitation density.[31]

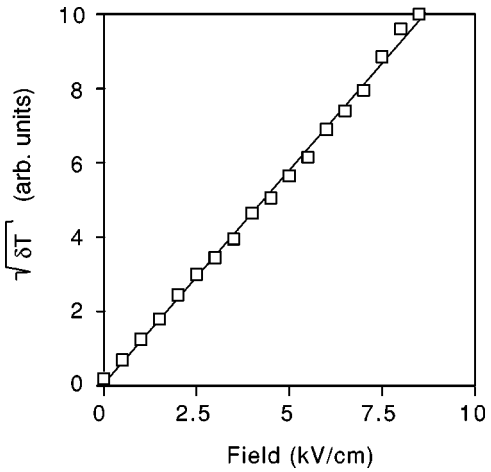

FIG. 8. Dependence of the EPA signal at 0.35 eV on the electric field.

IV. ELECTROMODULATION SPECTROSCOPY OF POLYTHIOPHENE DERIVATIVES

A. P3OT

The PA and EPA spectra of C_{60}-doped P3OT are shown in Fig. 9(a). Both spectra consist of a band below 0.8 eV, a second band at 1.25 eV, and a third band at 1.7 eV. The signal above 1.8 eV is due to a combination of electroabsorption and thermal effects. The resemblance of the spectra to those shown in Fig. 4 for MEH-PPV/C_{60} suggests the same assignments as before, i.e., two PA bands due to polaron

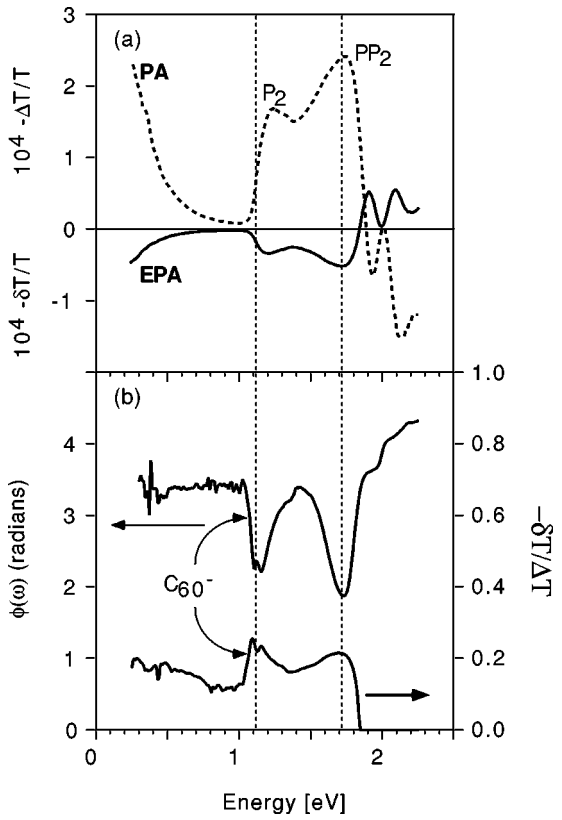

FIG. 9. (a) Comparison between the PA and the EPA signal in P3OT/C_{60}. (b) The phase of the EPA signal and the relative sensitivity of the photoexcitations indicate two related transitions at 1.15 and 1.7 eV.

pairs (0.4 and 1.7 eV) and one PA band due to C_{60}^-. The discrepancy between the PA band at 1.25 eV and the PA of C_{60}^- in MEH-PPV/C_{60} suggests that this is not the case. A more complete analysis of the data includes the phase of the EPA spectrum and the relative sensitivity of the photoexcitations to an electric field. Since the phase of the signal is sensitive to the lifetime of excitations, it can be used to correlate bands that belong to the same excitation. The relative sensitivity of the PA bands to an electric field ($\delta T/\Delta T$) serves the same purpose. We apply both of these analysis techniques to the PA and EPA of C_{60}-doped P3OT as the presence of multiple overlapping bands means that EPA alone is insufficient to separate the excitations.

The spectra of the EPA phase and the ratio of the EPA ($\delta T/\Delta T$) and PA are shown in Fig. 9(b). The absorption band of C_{60} anions at 1.15 eV is visible in both spectra.[37,40] While the PA band at 1.7 eV is correlated with the C_{60}^- band, the bands below 0.5 eV and at 1.25 eV are clearly not. We therefore identify the band at 1.7 eV as the higher-energy band of the positive component of the polaron pairs. This leaves the PA bands at below 0.5 eV and at 1.25 eV. These bands are not correlated with the lifetimes of the P^+/C_{60}^- complexes, but are sensitive to an applied electric field [Fig. 9(a)]. In two recent papers, we showed that the PA spectrum of polarons in π-conjugated polymers consists of two bands[36] and that the high-energy polaron pair PA band is blueshifted with respect to the high-energy polaron PA band.[14] We therefore assign these two PA bands to isolated polarons (Figs. 1 and 9).

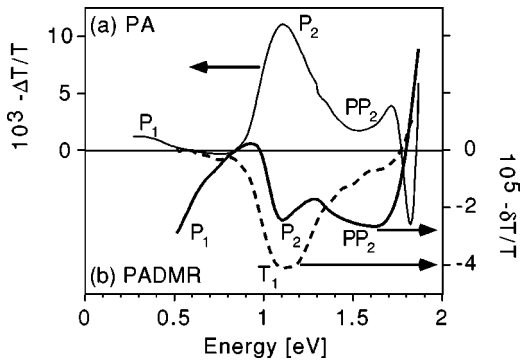

FIG. 10. (a) The PA spectrum of PTSi. (b) The spin-1/2 (solid line) and spin-1 (dashed line) PADMR spectra of PTSi.

B. PTSi

The PA spectrum of pristine PTSi [Fig. 10(a)] is dominated by a broad band between 0.9 and 1.4 eV with a peak at 1.1 eV; PA extends up to 1.8 eV and there is also a distinctive band at 0.3 eV. We attribute the sharp zero-level crossing at 1.8 eV to electroabsorption from charged photoexcitations as before. The PA between 0.9 and 1.8 eV contains contributions from optical transitions of triplet excitons, polaron pairs, and free polarons. PADMR spectroscopy permits us to decompose the PA spectrum into its constituent parts. The PADMR spectrum of triplet excitons [Fig. 10(b)], measured with the magnetic field set to the half-field resonance at 500 G, has a single band with a maximum at 1.1–1.2 eV and extending up to 1.8 eV. The spin-1/2 PADMR spectrum [Fig. 10(b)], measured at G, contains bands at 1.1 and 1.7 eV as well as a band below 0.5 eV. The cryostat windows did not permit measurements below 0.4 eV. In accord with our conclusions on PA and EPA in P3OT, we attribute the band at 1.1 eV to polarons (P_2), the band at 1.7 eV to polaron pairs (PP_2), and the band below 0.8 eV to a combination of polarons and polaron pairs (P_1+PP_1). The weak positive PADMR between 0.9 and 1.0 eV is probably due to spinless bipolarons.[36] Comparison of the PA and PADMR spectra shows that the PA spectrum of PTSi is dominated by triplet excitons, though not to the degree of MEH-PPV.

The EPA spectrum of pristine PTSi is shown in Fig. 11. We were able to detect an EPA spectrum of undoped PTSi, possibly because its PA is an order of magnitude stronger than that of MEH-PPV (Fig. 4). The EPA spectrum of PTSi is quite different than that observed previously; the electric field generally enhances the PA intensity and so we must

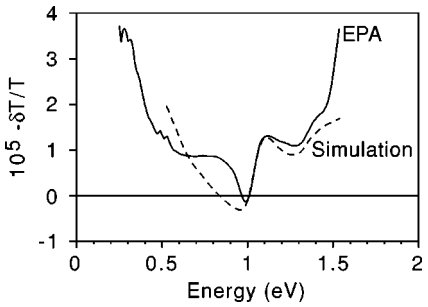

FIG. 11. The EPA spectrum of PTSi (solid line) and a simulation of the EPA spectrum (dashed line). The simulation is the difference between the polaron and triplet PADMR spectra.

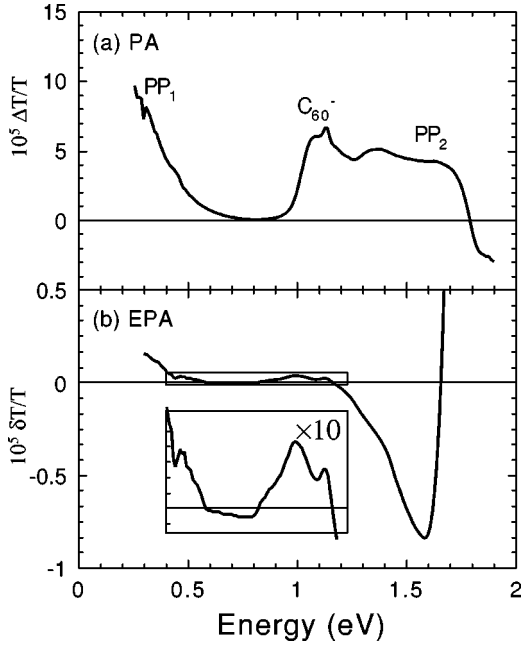

FIG. 12. (a) The PA spectrum of PTSi/C_{60}. (b) The EPA spectrum of PTSi/C_{60}. The inset shows the EPA on a magnified vertical scale.

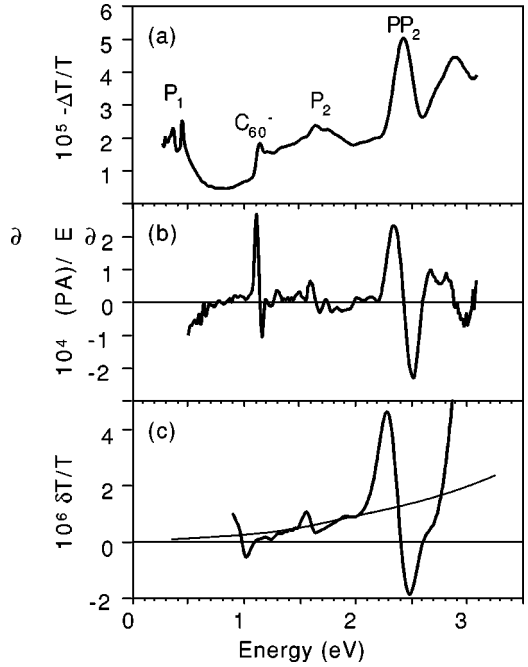

FIG. 13. (a) The PA spectrum of PPP/C_{60}. (b) The derivative of the PA signal with respect to energy. (c) The EPA spectrum of PPP/C_{60}.

find a different explanation than field-induced tunneling. A fairly good simulation of the EPA spectrum can be generated by taking the difference between the spin-1/2 and triplet PADMR spectra ($\delta T_{\mathrm{sim}} = \delta T_{S=1/2} - \delta T_{S=1}$) and is shown as a dashed line in Fig. 11. The electric field thus appears to enhance the steady state population of polarons and polaron pairs which, in turn, reduces the steady state population of triplet excitons. The discrepency between the fit and the measured EPA spectrum may arise from contributions of bipolarons to the PADMR spectrum.[36]

We suggest that the EPA signal is due to field-induced enhancement of singlet exciton dissociation into polarons and polaron pairs. This has two effects: (i) the fraction of the singlet excitons that may decay into the triplet manifold is reduced and (ii) the number of polarons and polaron pairs is increased. Hence, the PA of triplet excitons is decreased and that of polarons and polaron pairs is enhanced. The agreement between the EPA spectrum and the simulated spectrum composed of the difference of the triplet and doublet PA (Fig. 11) can be explained this way. This hypothesis is supported by our observation that simultaneously the PL intensity is reduced by an electric field. At a field of 10^5 V/cm, the PL is reduced by a factor of 5×10^{-4}.[31] For our field strengths, similar reduction were not seen for MEH-PPV or P3OT. Due to high exciton binding energies, electric field enhanced dissociation of excitons happens close to impurities that tend to dissociate excitons to form charge transfer complexes.

The PA spectrum of PTSi/C_{60} is shown in Fig. 12(a). The spectrum closely resembles that of the spin-1/2 PADMR spectrum of PTSi [Fig. 10(b)] and can be attributed to charged photoexcitations. The sharp PA signature of C_{60} anions at 1.15 eV is also visible. If present, the PA signature of triplet excitons is weak. The EPA spectrum of PTSi/C_{60} [Fig. 11(b)] is quite different from that of PTSi. There are positive bands below 0.5 eV and between 0.8 and 1.2 eV and a very strong negative band with a maximum at 1.6 eV. The signature of C_{60}^- is seen in the positive band, indicating that the effect of the electric field is to increase the C_{60}^- density. Taking the PA band at 1.7 eV as due to polaron pairs, these results suggest that the density of polaron pairs is reduced by an electric field while that of polarons and C_{60}^- is increased by an electric field. This is consistent with the results on pristine PTSi (exciton dissociation at defects such as fullerene dopants) and on MEH-PPV/C_{60} (electric field assisted tunneling).

V. STARK SHIFT OF CHARGE TRANSFER COMPLEXES IN C_{60}/RO-PPP

Figure 13 compares (a) the PA spectrum, (b) the derivative of the PA spectrum, and (c) the EPA spectrum of RO-PPP/C_{60}. As can be seen in Fig. 13(a) the PA of RO-PPP/C_{60} shows distinct features at 0.5, 1.1, 1.7, and 2.4 eV. We assign the PA band at 1.1 eV to C_{60}^- and the remaining PA bands to polarons and polaron pairs as above. Figure 13(b) shows the derivative of the PA signal with respect to the energy. The EPA signal shows spectral features that resemble the PA derivative roughly 0.1 eV below each of the respective spectral features in the PA [Fig. 13(c)]. The derivativelike shape is a clear indication that the EPA spectrum is dominated by a Stark shift of the state energies rather than changes in the photoexcitation lifetimes. The gradually sloping line in Fig. 13(c) is to provide a zero line for the derivative interpretation. The PA band at 2.4 eV and the related derivative shaped feature in the EPA spectrum is due to the absorption of the positive polaron bound to the C_{60} counterion (P^+/C_{60}^-). Unlike in MEH-PPV/C_{60}, the electric field causes a significant redshift of the polaron pair absorption signature. Since the features in the EPA spectrum are shifted

in energy below the respective features of the PA signal, then we conclude that the longer conjugation lengths of the polymer dominate the EPA spectrum. This effect is known for EA spectra, which are proportional to the imaginary component of the third-order dc nonlinear optical susceptibility $\chi^{(3)}(-\omega;\omega,0,0)$.[6]

We can calculate the polarizability α_P of the (P^+/C_{60}^-) charge-transfer complex from the PA and EPA spectra. This calculation is performed similarly to the calculation of α_P for the $1B_u$ exciton.[31,41] In order to ensure the same number of photoexcitations during the PA and EPA measurement for both spectra, the film thickness and the illumination intensity must be the same for both measurements. For the PA measurement, the modulation period $1/f$ must be much smaller than the photoexcitation lifetime so that the PA signal reflects the photoexcitation density. The EPA signal δT is related to the PA signal ΔT by

$$\delta T(\omega)=\Delta T(F,\omega)-\Delta T(0,\omega), \tag{11}$$

where ω is the state energy. If a Stark shift is the only relevant modification of the spectral PA signal due to an electric field, we can write

$$\Delta T(F,\omega)=\Delta T(0,\omega+\Delta E), \tag{12}$$

where ΔE is the Stark shift of the excitation energy due to an electric field F,

$$\Delta E=-m_iF_i+p_{ij}F_iF_j, \tag{13}$$

where m_i is the permanent dipole moment and p_{ij} the polarizability tensor. Taking the difference between the PA signals with and without the applied fields yields the following:

$$\delta T(\omega)=\Delta T(\omega+\Delta E)-\Delta T(\omega)\approx\frac{\partial(\Delta T)}{\partial E}\Delta E \tag{14}$$

to lowest order. The photoexcitations are randomly oriented so the average Stark shift due to $\vec{m}$ cancels out but broadens the PA band when an electric field is applied. This additional broadening can be neglected as the PA itself is quite broad due to the conjugation length distribution. We can then write

$$\Delta E=\frac{1}{2}\alpha_pF^2. \tag{15}$$

The photoexcitation polarizability can be calculated from EPA and PA analogously to the polarizability of the $1B_u$ exciton[6,30] as

$$\delta\alpha d=-\frac{\delta T}{T}=\frac{7}{60}\alpha_PF^2\frac{\partial}{\partial E}\left(-\frac{\Delta T}{T}\right). \tag{16}$$

The factor 7/60 is a result of the averaging over different orientations in space. This simplified analysis cannot be applied carelessly to the EPA spectrum. The modulation of the photoexcitation lifetime due to an electric field contributes to the signal and obscures the Stark shift. In addition, the presence of mobile charge carriers leads to Thomas Fermi screening. Thus the electric field is not continuously distributed between the electrodes, but larger close to the electrodes and smaller further away. Therefore the information obtained will only give an order of magnitude estimate of the photoexcitation polarizability.We divided the EPA spectrum by the derivative of the PA spectrum and calculated the change in α_P to be approximately 3×10^7 Å^3. This is approximately 200 times larger than the polarizability change between the $1A_g$ and $1B_u$ states of most luminescent π-conjugated polymers. As α_P of the ground state is of order 10^4 Å^3, α_P of charge-transfer complexes in C_{60}-doped RO-PPP is roughly the polarizability difference. From α_P one may calculate the diameter of the charge-transfer complex $a\cong\sqrt[3]{\alpha_P/4\pi}$. We find that a is approximately 10 nm, which is six times larger than a of the $1B_u$ exciton.

VI. CONCLUSIONS

EPA is a technique used to investigate photoexcitations in conjugated polymers. An electric field was found to have three major effects on photoexcitations in conjugated polymers and polymer/ C_{60} blends.

(1) The lifetime of charge-transfer complexes was reduced by an applied electric field. We developed a model for electromodulation of the tunneling probability of the negative charge on the C_{60} anion back to the polymer chain. In combination with PA and PADMR spectroscopy, we measured the energies of PA bands associated with polarons, polaron pairs, and triplet excitons in all the systems studied.

(2) An electric field can enhance the dissociation of the 1Bu singlet excitons. This effect decreases the PL intensity, increases the populations of polarons and polaron pairs, and decreases the triplet exciton population. The effect dominates the EPA spectrum of PTSi.

(3) A Stark shift of charge-transfer complexes dominates the EPA spectrum of RO-PPP/C_{60} blends. The derivative shaped spectrum allows for the calculation of the difference in polarizability between ground and excited state of charge transfer excitations. The charge transfer complex is roughly 10 nm in diameter.

ACKNOWLEDGMENTS

We would like to thank the following individuals for generously supplying the conjugated polymers studied in this work: Z. Kafafi for MEH-PPV, M. Hamaguchi, M. Ozaki, and K. Yoshino for RO-PPP, T. J. Barton for PTSi, and D. Moses for P3OT. We would also like to thank C. Taliani, S. J. Martin, and Z. Kafafi for useful discussions. This project was supported by the U.S. Department of Energy, Grant No. FG-03-96 ER 45490, and the European Grant No. TMR/SELOA.

*Present address: I.U.T. GmbH, Rudower Chaussee 5, 12489 Berlin-Adlershof, Germany.

[1] L. Sebastian and G. Weiser, Chem. Phys. Lett. **64**, 396 (1979); Chem. Phys. **62**, 447 (1981); Phys. Rev. Lett. **62**, 1156 (1981).

[2] G. Weiser, Phys. Rev. B **45**, 14 076 (1992).

[3] J. M. Leng, S. Jeglinski, X. Wei, R. E. Benner, Z. V. Vardeny, D. Guo, and S. Mazumdar, Phys. Rev. Lett. **72**, 156 (1994).

[4] O. M. Gelsen, D. D. C. Bradley, H. Murata, N. Takada, T. Tsutsui, and S. Saito, J. Appl. Phys. **71**, 1064 (1992).

[5] D. A. Halliday, P. L. Burn, D. D. C. Bradley, R. H. Friend, O. M.

Gelsen, A. B. Holmes, A. Kraft, J. H. F. Martens, and K. Pichler, Adv. Mater. **5**, 40 (1993).
[6] M. Liess, S. Jeglinski, Z. V. Vardeny, M. Ozaki, K. Yoshino, Y. Ding, and T. J. Barton, Phys. Rev. B **56**, 5781 (1997).
[7] R. Kersting, U. Lemmer, M. Deussen, H. J. Bakker, R. F. Mahrt, H. Kurz, V. I. Arkhipov, H. Bässler, and E. O. Göbel, Phys. Rev. Lett. **73**, 1440 (1994).
[8] R. F. Code, Z. D. Popovic, and J. H. Sharp, Chem. Phys. **83**, 181 (1984).
[9] M. Esteghamatian, Z. D. Popovic, and G. Xu, J. Phys. Chem. **100**, 13 716 (1996).
[10] M. Deussen, P. H. Bolivar, G. Wegmann, H. Kurz, and H. Bassler, Chem. Phys. **207**, 147 (1996).
[11] M. C. J. M. Vissenberg and M. M. M. de Jong, Phys. Rev. Lett. **77**, 4820 (1996); Phys. Rev. B **57**, 2667 (1998).
[12] E. M. Conwell, Phys. Rev. Lett. **78**, 4301 (1997).
[13] X. Wei, B. C. Hess, Z. V. Vardeny, and F. Wudl, Phys. Rev. Lett. **68**, 666 (1992).
[14] P. A. Lane, X. Wei, and Z. V. Vardeny, Phys. Rev. B **56**, 4626 (1997).
[15] P. A. Lane, M. Liess, X. Wei, S. Frolov, Z. V. Vardeny, and Z. H. Kafafi, Proc. SPIE **2854**, 102 (1997).
[16] M. Liess, P. A. Lane, Z. V. Vardeny, and Z. Kafafi, Synth. Met. **84**, 683 (1997).
[17] Y. Wang, Nature (London) **356**, 585 (1992).
[18] N. S. Sariciftci, L. Smilowitz, A. J. Heeger, and F. Wudl, Science **258**, 1474 (1992).
[19] S. Morita, A. A. Zakhidov, and K. Yoshino, Solid State Commun. **82**, 249 (1992).
[20] L. Smilowitz, N. S. Sariciftci, R. Wu, C. Gettinger, A. J. Heeger, and F. Wudl, Phys. Rev. B **47**, 13 835 (1993).
[21] B. Kraabel, C. H. Lee, D. McBranch, D. Moses, N. S. Sariciftci, and A. J. Heeger, Chem. Phys. Lett. **213**, 389 (1993).
[22] N. S. Sariciftci and A. J. Heeger, Int. J. Mod. Phys. B **8**, 237 (1994).
[23] J. Bruening and B. Friedman, J. Chem. Phys. **106**, 9634 (1997).
[24] X. Wei, Ph.D. thesis, University of Utah, 1992.
[25] D. Beljonne, Z. Shuai, and J. L. Brdas, J. Chem. Phys. **98**, 8819 (1993).
[26] P. A. Lane, X. Wei, Z. V. Vardeny, J. Poplawski, E. Ehrenfreund, M. Ibrahim, and A. J. Frank, Chem. Phys. **210**, 229 (1996).
[27] V. Berger, N. Vodjdani, B. Vinter, E. Costard, and E. Boeckenhoff, Appl. Phys. Lett. **60**, 1869 (1992).
[28] Z. V. Vardeny and X. Wei, in *Handbook of Conducting Polymers*, edited by A. Skotheim, R. Elsenbaumer, and R. L. Reynolds (Marcel-Dekker, NY, 1997), Chap. 22, pp. 639–666.
[29] S. Frolov, Ph.D. thesis, University of Utah, 1997.
[30] S. Jeglinski, Ph.D. thesis, University of Utah, 1997.
[31] M. Liess, Ph.D. thesis, University of Utah, 1997.
[32] R. I. Devlen, G. S. Kanner, Z. V. Vardeny, and J. Tauc, Solid State Commun. **78**, 665 (1991).
[33] G. Yu, J. Gao, J. C. Hummelen, F. Wudl, and A. J. Heeger, Science **270**, 1789 (1995).
[34] X. Wei, Z. V. Vardeny, N. S. Sariciftci, and A. J. Heeger, Phys. Rev. B **53**, 2187 (1996).
[35] K. F. Voss *et al.*, Phys. Rev. B **49**, 5781 (1991).
[36] P. A. Lane, X. Wei, and Z. V. Vardeny, Phys. Rev. Lett. **77**, 1544 (1996).
[37] K. Lee, R. A. J. Janssen, N. S. Sariciftci, and A. J. Heeger, Phys. Rev. B **49**, 5781 (1994).
[38] J. M. Warman *et al.*, Proc. SPIE **3145**, 142 (1997).
[39] L. S. Swanson, P. A. Lane, J. Shinar, and F. Wudl, Phys. Rev. B **44**, 10 617 (1991).
[40] S. Luzzati, F. Speroni, Anvar Zakhidov, S. Morita, and K. Yoshino, Mol. Cryst. Liq. Cryst. **256**, 927 (1994).
[41] S. Jeglinski, Z. V. Vardeny, Y. Ding, and T. Barton, Mol. Cryst. Liq. Cryst. **256**, 87 (1994).